Dynamics of G-quadruplex oligonucleotide sequences as affected by complexation with pharmaceutical molecules

Student: Luca Bertini

Tutors:
Dr. Lucia Comez (CNR-IOM)
Prof. Alessandro Paciaroni (UNIPG)

Educational activities (courses)

- **Introduction to Effective Field Theory (EFT);**
- **Probability and uncertainty in measurements;**
- **Nanosystems and advanced materials;**
- **Introduction to Atmospheric Physics, Climate and COPERNICUS DATA STORE (CDS)**
- **Multimessenger Astrophysics – from EM multifrequency to gravitational waves;**
- **Teaching and Learning Physics at University;**
- **Physics at LHC;**
- **Formazione trasversale ai dottorandi (2020).**

Educational activities (seminars)

- **Perugia Advanced Physics (Cycle);**
- **Soft X-ray Spectroscopies for liquids;**

Publications

- **“The role of fast dynamics in G-quadruplex complexation with small molecules”, Bertini et al. (in preparation)**

G-quadruplex

- **G-quadruplex** (G4) is a non-canonical secondary structure formed by stacking of **G-tetrads** on top of one another. G-tetrads are formed by four guanines linked via **Hoogsteen bonds**. The remaining bases in the strand form **loops** connecting the tetrads and the whole structure is stabilized by the presence of a **positive ion** (either K^+ or Na^+)

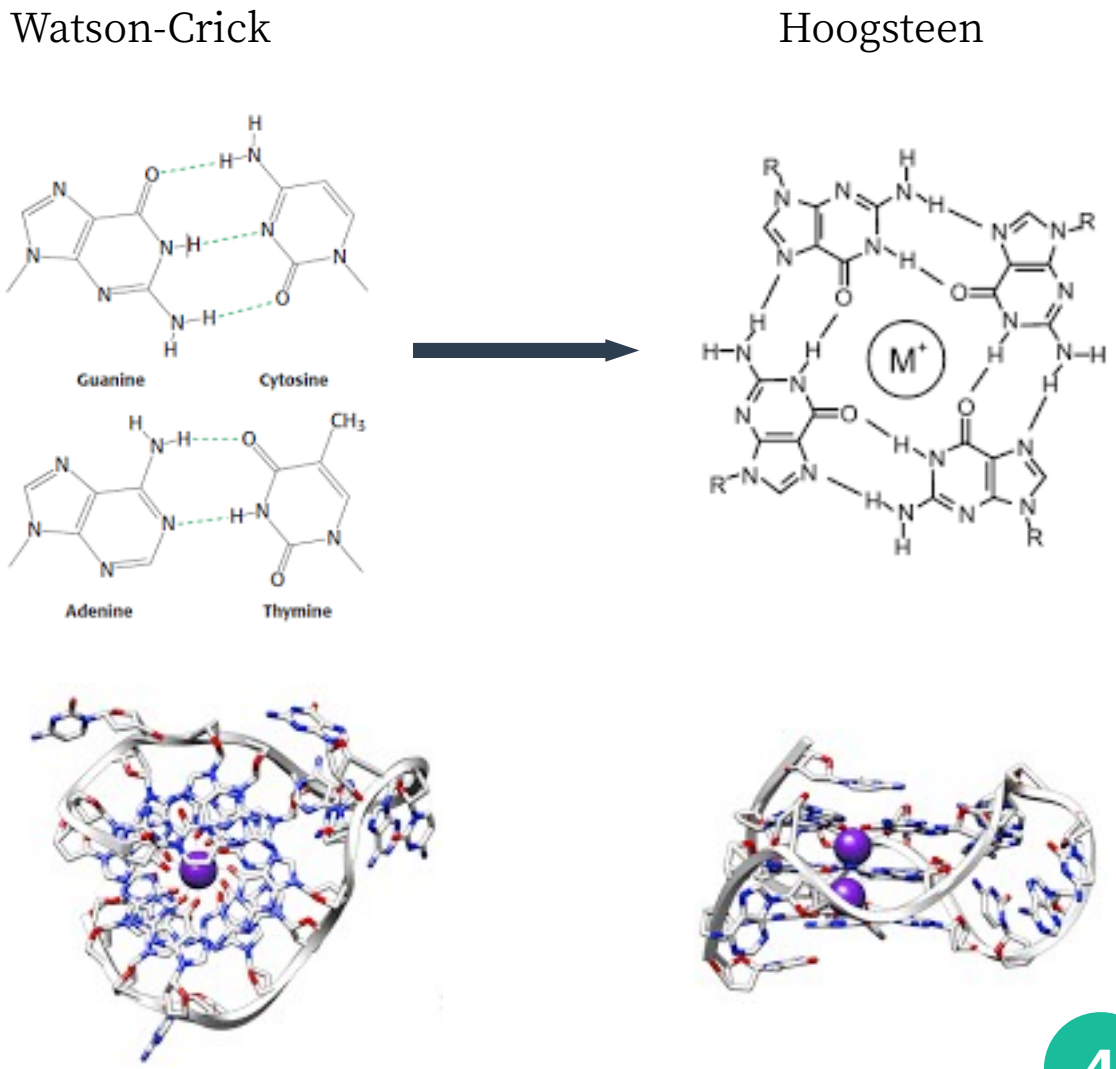

Telomeric G-quadruplexes

G-rich oligonucleotide sequences in the terminal parts of **telomeres** are prone to form G-quadruplex structures in the presence of cations such as K+ and Na+. **Polymorphysm** is a main feature of these structures, whose **stabilization** is highly desirable to promote **telomerase inhibition** in cancer cells. Ligand induced stabilization is then a matter of growing interest in the scientific community.

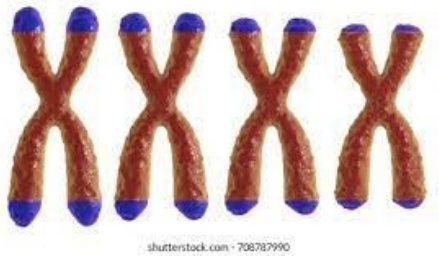

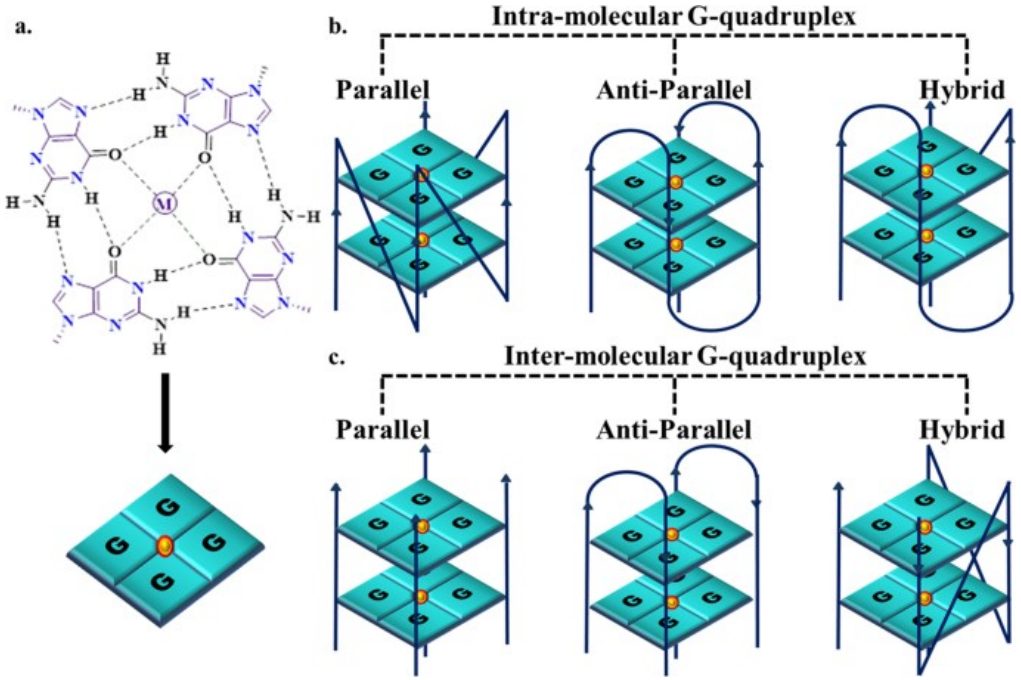

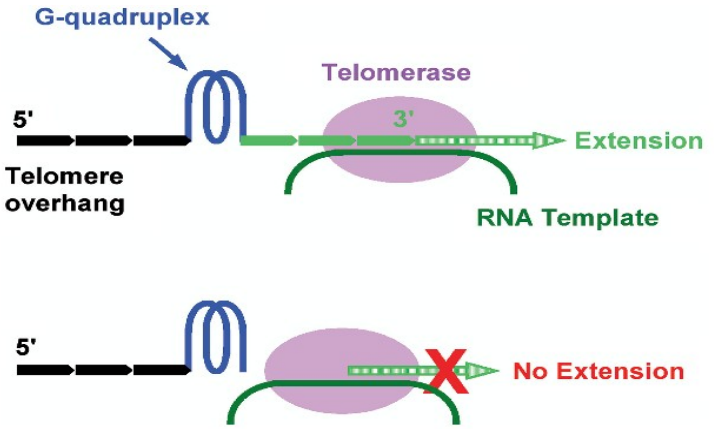

G-rich oligonucleotides

G-quadruplexes are also found in promoter regions of some genes, possibly playing an important role in gene regulation. In this case G-quadruplex stabilization could be used to achieve either upregulation or downregulation.
A notable example is the presence of G4 in some proto-oncogenes that are found in the human genome[1].
RNA sequences can also form G4 structures, as suggested by a recent study on SARS-CoV-2 genome, thus proving as a valuable target for antiviral drugs[2].

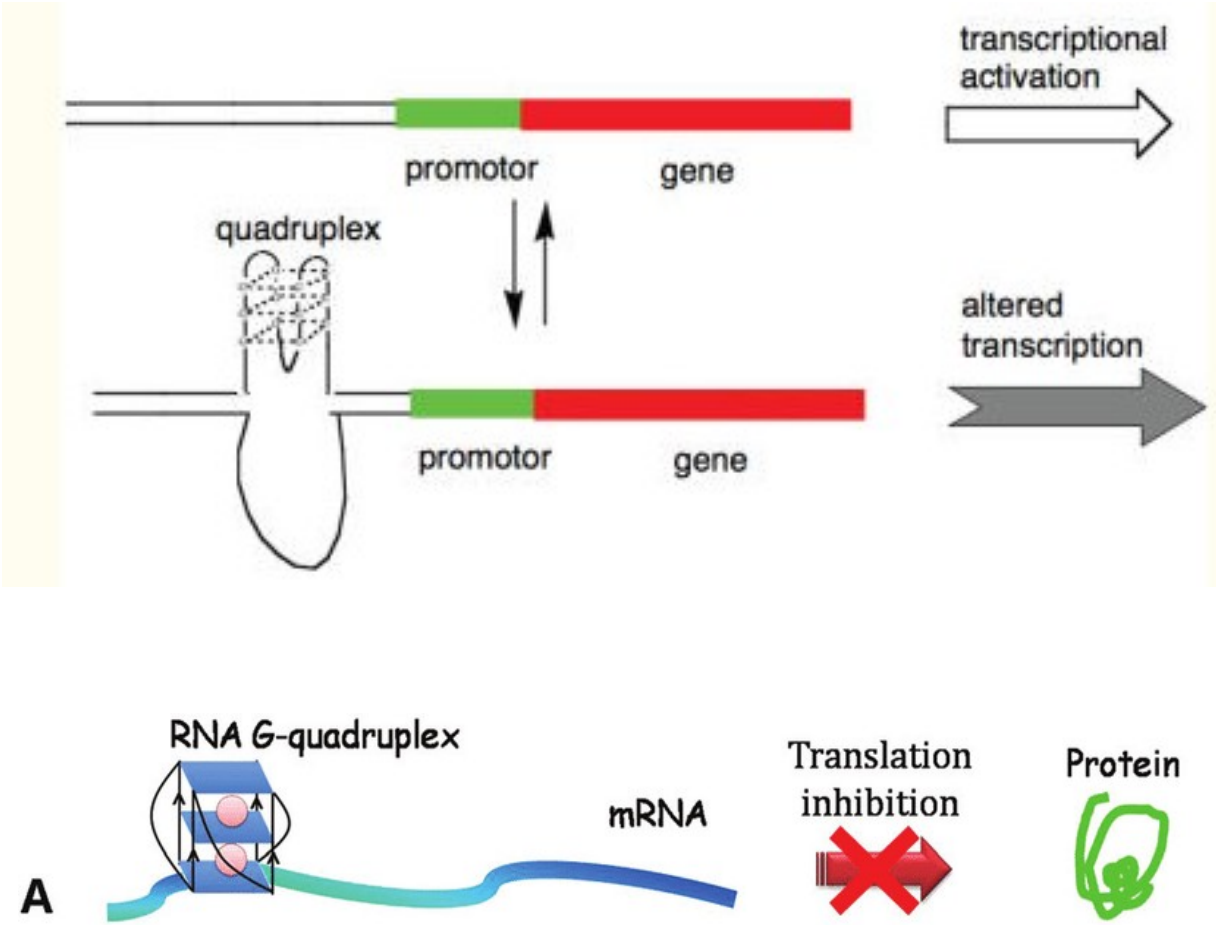

Small ligands: BRACO19 and Berberine

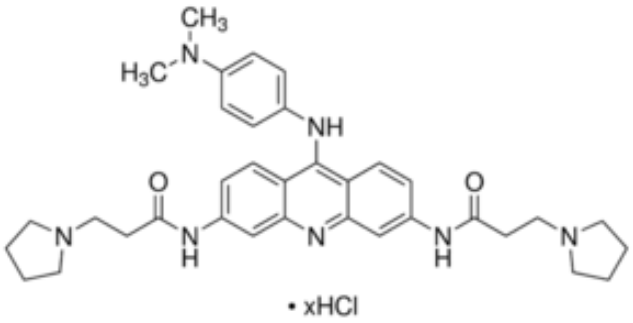

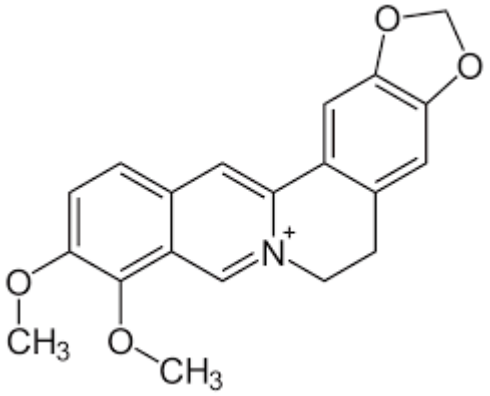

- BRACO19 is a trisubstituted acridine that has been shown to act as a moderate telomerase inhibitor;
- High affinity with Tel22 G4 in presence of K^+.

- Berberine is a natural quaternary ammonium salt characterized by low systemic toxicity and anticancer activity;
- High G4 affinity, but low selectivity.

Neutron Scattering

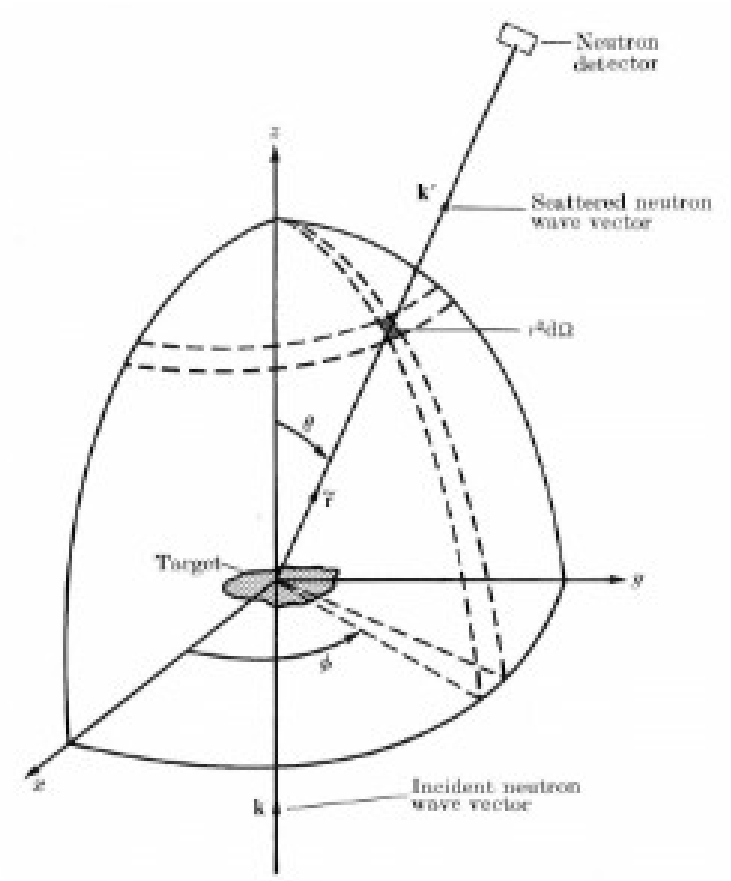

- Cold neutrons have energies of ~meV and wavelengths of ~$Å^{-1}$ matching both spatial- and time- scales of relevant molecular motions in biological systems such as G4, giving access to both geometrical and dynamical information;
- In these experiments we only consider the nuclear interaction with matter: cross-sections are isotope dependent;
- Hydrogen contribution to the total cross section is predominant and mainly incoherent.

Incoherent Neutron Scattering

The differential cross-section can be written in terms of the **structure factor** as:

$$\frac{\mathrm{d}^2\sigma}{\mathrm{d}\Omega\,\mathrm{d}\omega} = \frac{k}{k_0}\left[\frac{\sigma_{\mathrm{coh}}}{4\pi}S_{\mathrm{coh}}(\boldsymbol{Q},\omega) + \frac{\sigma_{\mathrm{inc}}}{4\pi}S_{\mathrm{inc}}(\boldsymbol{Q},\omega)\right]$$

In terms of the **correlation functions** we have:

$$S(\boldsymbol{Q},\omega) = (2\pi)^{-1}\int_{-\infty}^{+\infty}\int_{-\infty}^{+\infty} G(\boldsymbol{r},t)\mathrm{e}^{\mathrm{i}(\boldsymbol{Q}\boldsymbol{r}-\omega t)}\mathrm{d}\boldsymbol{r}\,\mathrm{d}t$$

$$S_{\mathrm{s}}(\boldsymbol{Q},\omega) = (2\pi)^{-1}\int_{-\infty}^{+\infty}\int_{-\infty}^{+\infty} G_{\mathrm{s}}(\boldsymbol{r},t)\mathrm{e}^{\mathrm{i}(\boldsymbol{Q}\boldsymbol{r}-\omega t)}\mathrm{d}\boldsymbol{r}\,\mathrm{d}t\ .$$

The correlation functions are the **space Fourier-transforms** of the **intermediate scattering fucnitons**:

$$I(\boldsymbol{Q},t) = N^{-1}\sum_{i=1}^{N}\sum_{j=1}^{N}\left\langle \mathrm{e}^{-\mathrm{i}\boldsymbol{Q}\boldsymbol{r}_i(0)}\mathrm{e}^{\mathrm{i}\boldsymbol{Q}\boldsymbol{r}_j(t)}\right\rangle \qquad I_{\mathrm{s}}(\boldsymbol{Q},t) = N^{-1}\sum_{i=1}^{N}\left\langle \mathrm{e}^{-\mathrm{i}\boldsymbol{Q}\boldsymbol{r}_i(0)}\mathrm{e}^{\mathrm{i}\boldsymbol{Q}\boldsymbol{r}_i(t)}\right\rangle$$

Incoherent Neutron Scattering

We may now write:

$$S_{\mathrm{s}}(\boldsymbol{Q},\omega) = (2\pi)^{-1} \int_{-\infty}^{+\infty} \int_{-\infty}^{+\infty} \mathrm{e}^{\mathrm{i}(\boldsymbol{Q}\boldsymbol{r}-\omega t)} [G_{\mathrm{s}}(\boldsymbol{r},\infty) + G'_{\mathrm{s}}(\boldsymbol{r},t)] \mathrm{d}\boldsymbol{r}\, \mathrm{d}t$$

$$S_{\mathrm{s}}(\boldsymbol{Q},\omega) = S_{\mathrm{s}}^{\mathrm{el}}(\boldsymbol{Q})\delta(\omega) + S_{\mathrm{s}}^{\mathrm{in}}(\boldsymbol{Q},\omega)$$

Finally, the finite resolution of the instrument is accounted for by convolution with the **resolution function**:

$$[S_{\mathrm{s}}(\boldsymbol{Q},\omega)]_{\mathrm{meas}} = \int_{-\infty}^{+\infty} S_{\mathrm{s}}(\boldsymbol{Q},\omega')R(\omega-\omega')\mathrm{d}\omega'$$

And contribution from harmonic motions is included by multiplication for the Debye-Waller factor:

$$W(\vec{Q}) = e^{-\frac{1}{6}\langle u^2\rangle Q^2}$$

EINS measurements

Both elastic and quasielastic measurements were performed at IN16b (ILL, Grenoble, France) on hydrated powder samples of Tel22 sequences both alone and in the presence of Berberine and BRACO19 ligands. EINS measurements with sub-μeV resolution tipically give access to information about vibrational motions taking place in the picosecond timescales. The atomic MSDs were retrieved by fitting the data with the function:

$$S(\vec{Q}) = a(\vec{q})e^{-\frac{1}{6}\langle u^2\rangle Q^2}$$

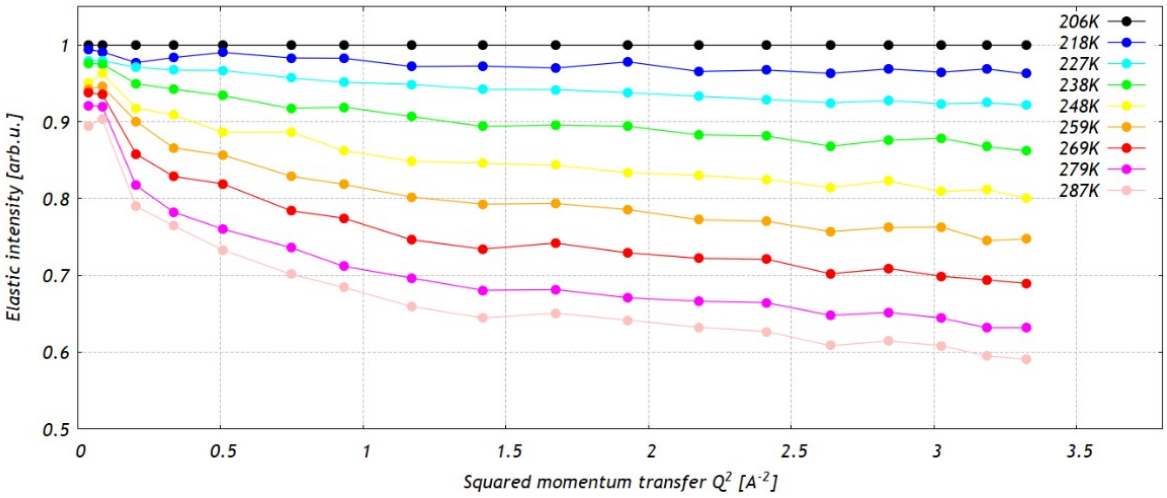

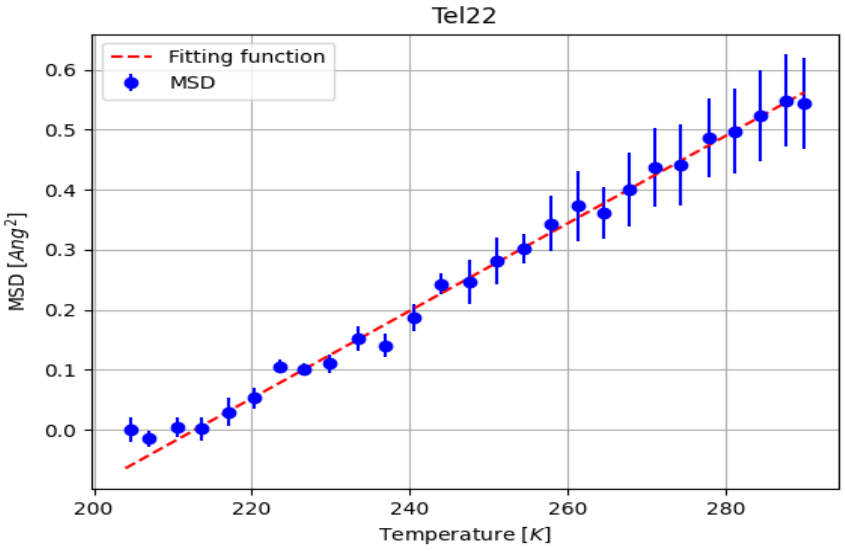

$$\langle u^2\rangle = \frac{3k_B}{k_{HT}}T$$

K_{HT}=59±2pNÅ^{-1}

EINS measurements

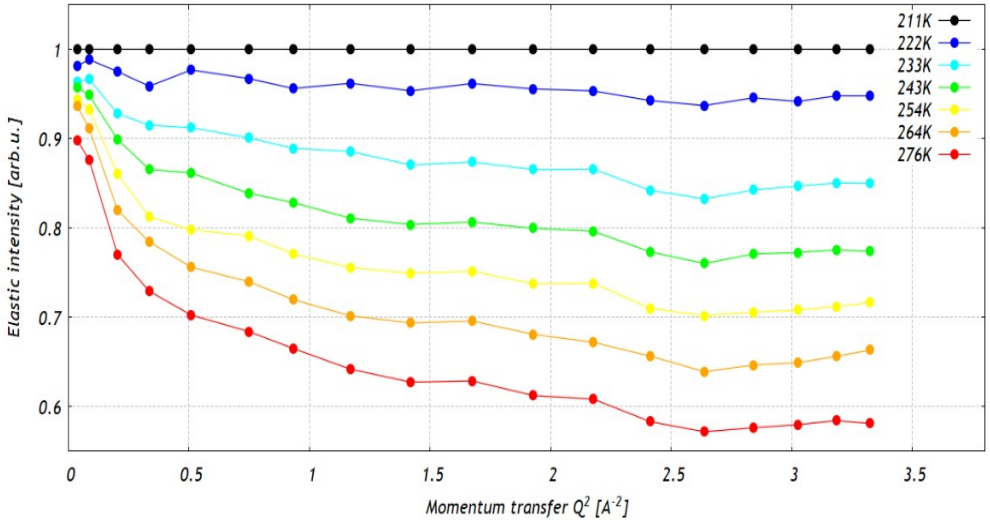

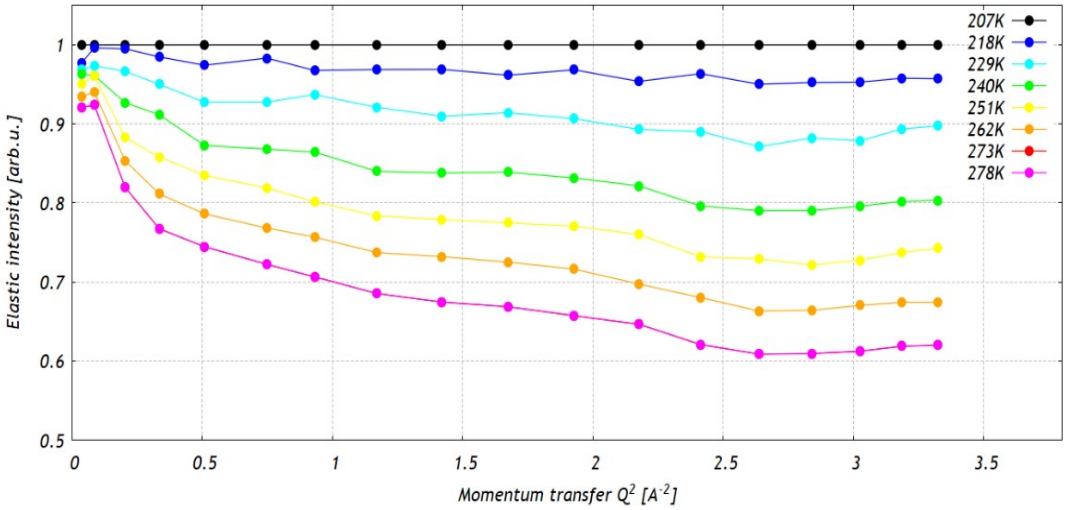

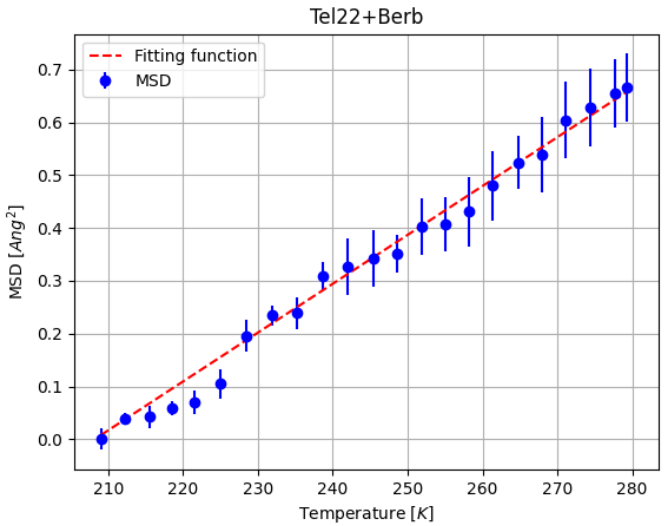

$K_{HT}=47\pm1 pN Å^{-1}$

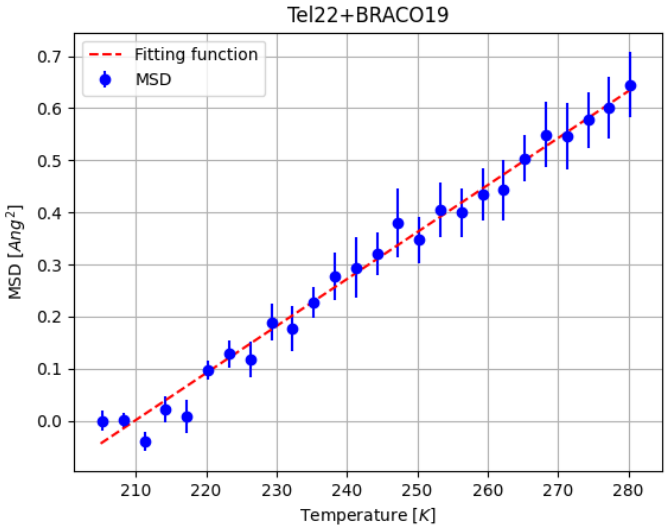

$K_{HT}=46\pm1 pN Å^{-1}$

EINS measurements

- It is evident from the data that complexation with the drugs results in increased mobility of the complex; this might be linked to an increase in entropy upon complexation; it was also demonstrated by CD measurements that conformational changes occur;
- An assessment of thermal stability may be attempted using a simple model (Einstein solid) to evaluate the force constant of the oscillators; the result for G4 is comparable to what has been obtained for mechanical stability assessments [3];

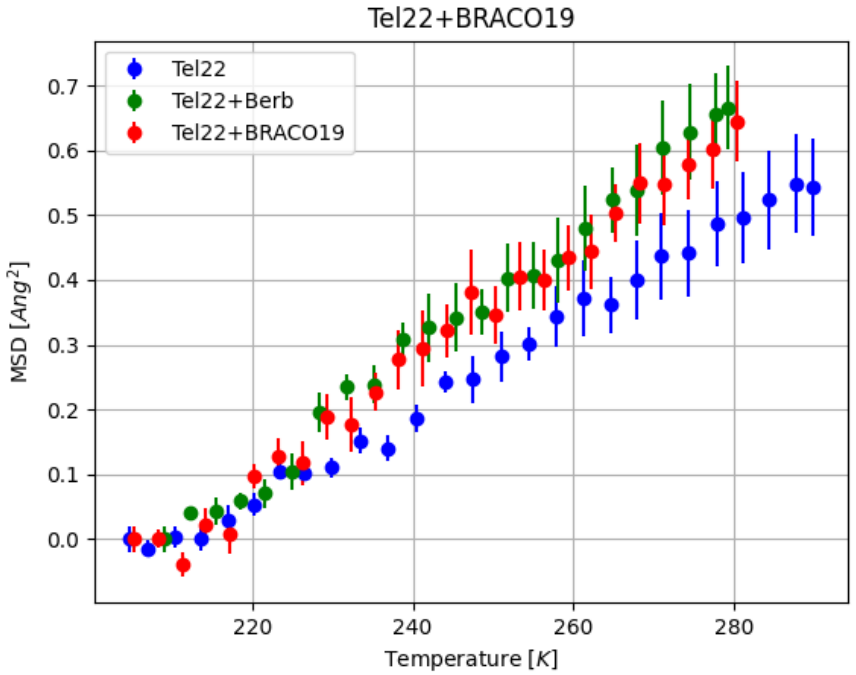

Entropy change[4]:

$$\Delta S = 3R \ln\left(\frac{u_c}{u_f}\right)$$

Conformational change upon complexation

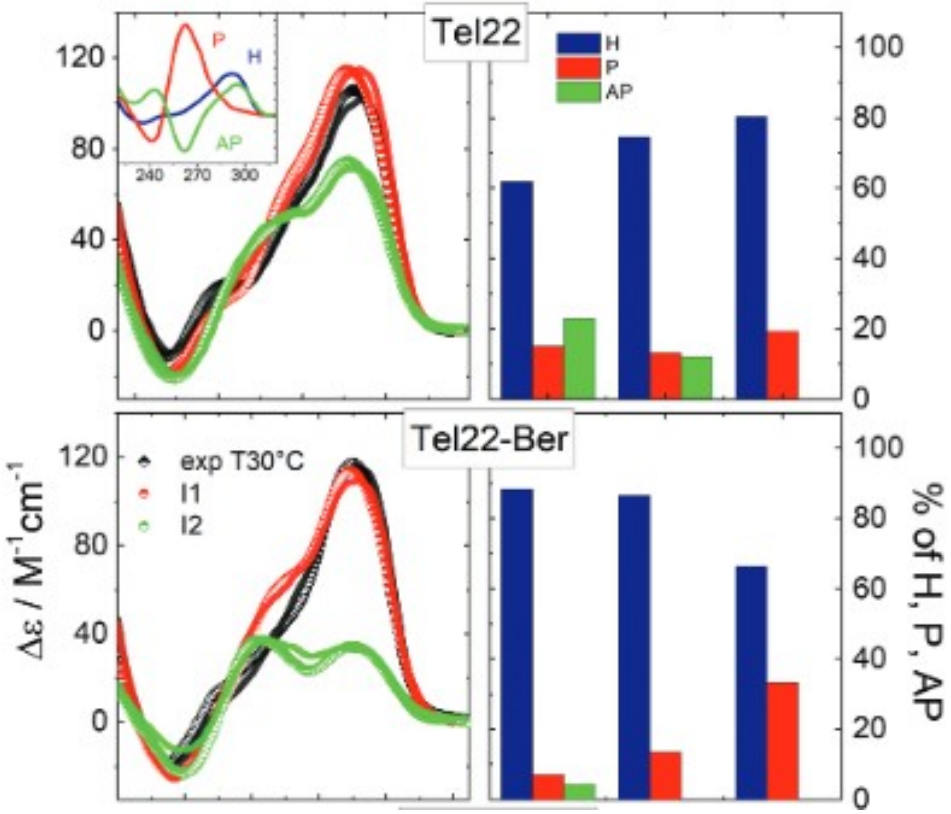

CD measurements on Tel22 and Tel22+Berberine samples (solution) show that percentage of hybrid conformation is increased upon complexation with respect to paralle and antiparallel conformations.

QENS measurements

The correlation functions can be estimated using well established models describing stochastic systems. In quasielastic neutron scattering we tipically have access to information concerning diffusion-like motions within the biomolecule. Confined random-jump diffusion models yields to expressions for the structure function containing an infinite series of lorentzian functions:

$$S_{\mathrm{inc}}(\mathbf{Q}, \omega) = \sum_{i=0}^{\infty} \sum_{j=0}^{\infty} \sum_{k=0}^{\infty} A_i(Q_x l) A_j(Q_y l) A_k(Q_z l) L(\Delta\omega_{ijk}),$$

$$\Delta\omega_{ijk} = \Gamma\{1 - \exp\,[-\tfrac{1}{2}(i^2 + j^2 + k^2)(\pi r_0/l)^2]\},$$

Different geometries for the confined motion can be taken into account, leading to similar expressions; the information on the geometry is contained in the $A_i(Ql)$ coefficients.

QENS measurements

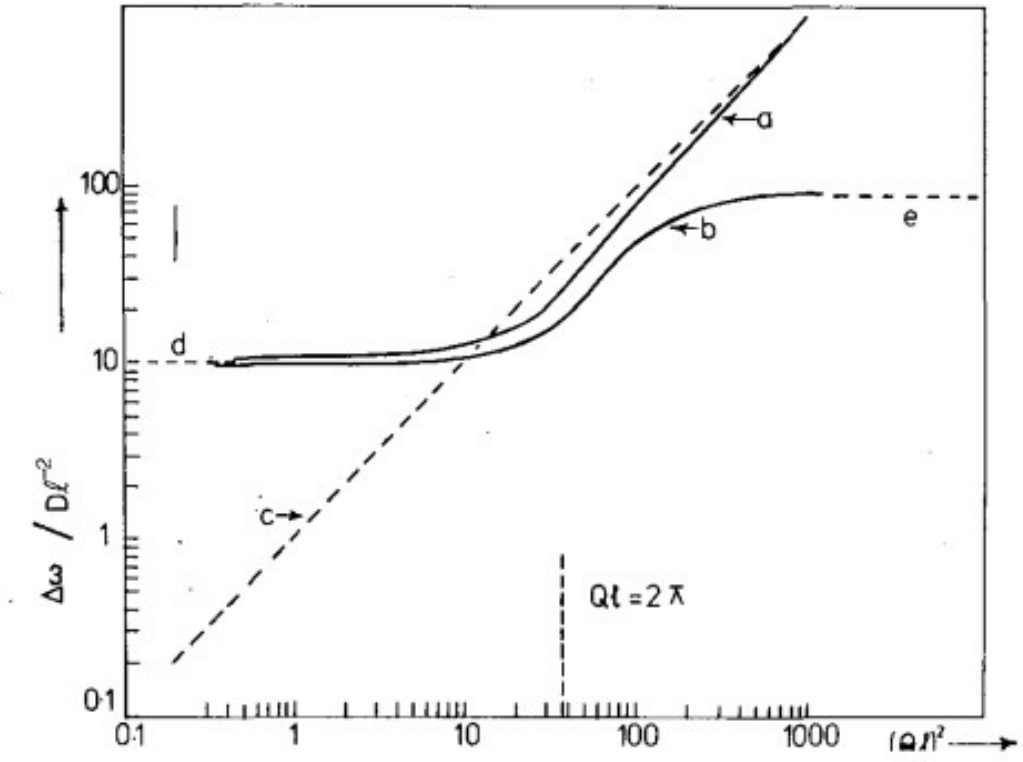

The nature of the diffusive motion can be readily determined by looking at the behaviour of the lorentzian broadening; deviations from the simple continuous unrestricted diffusion model can be found both at small and large values of Q

QENS spectra

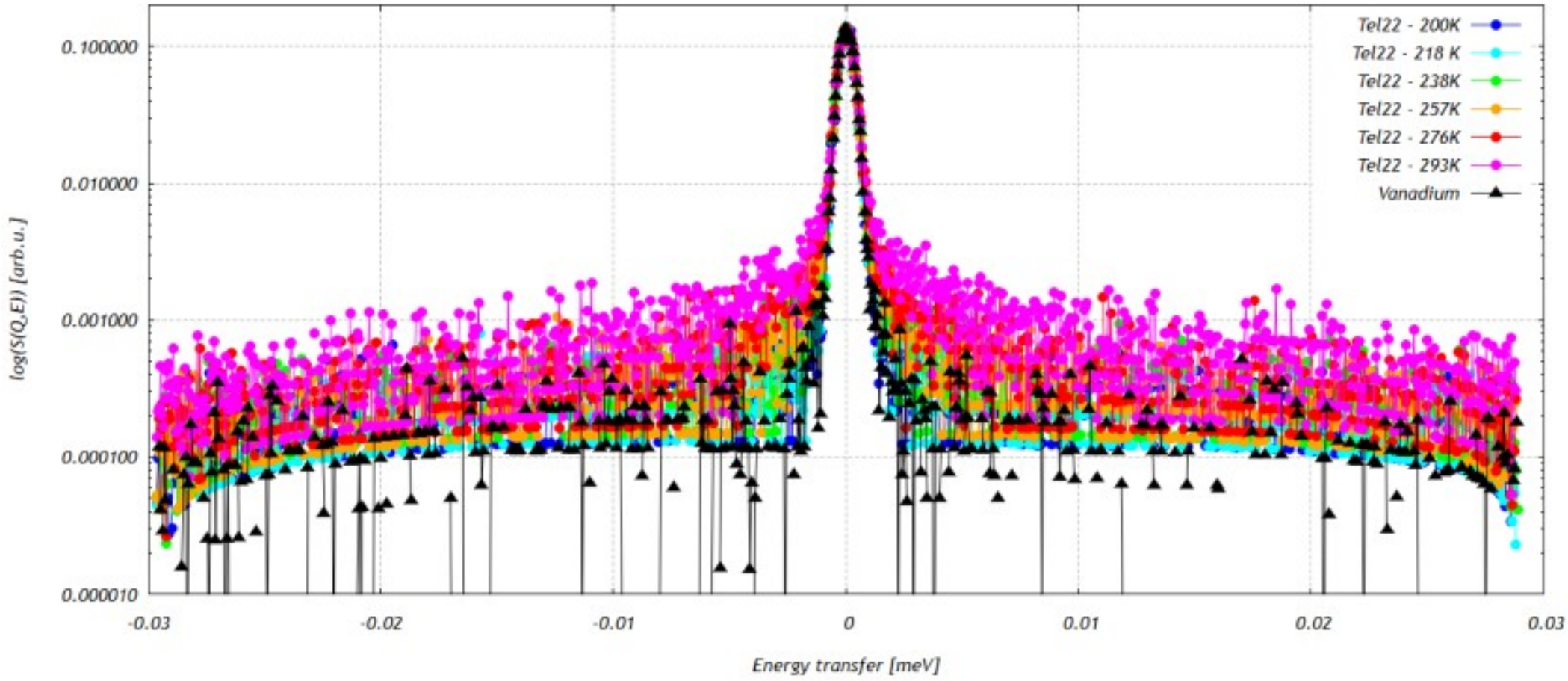

Tel22 QENS spectra at different temperatures

QENS spectra

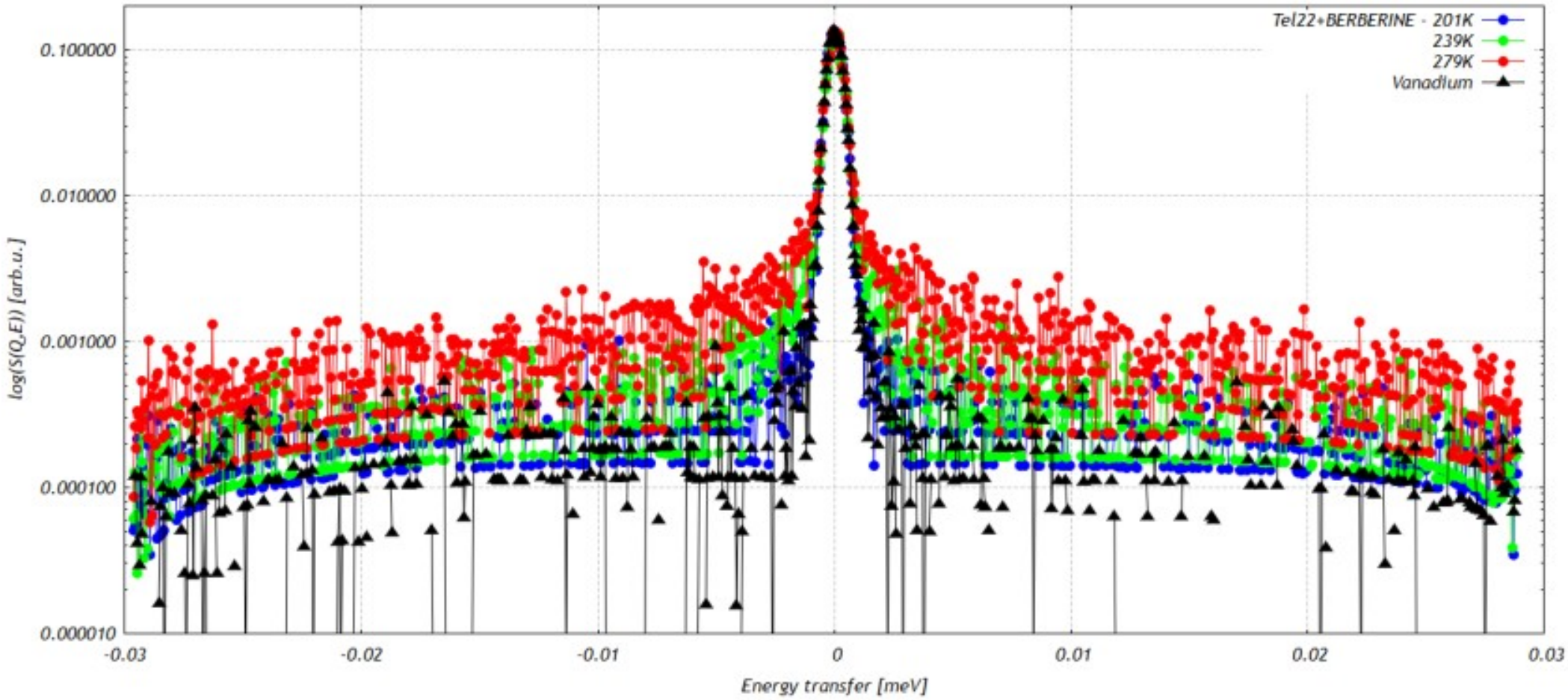

Tel22+berberine QENS spectra at different temperatures

QENS spectra

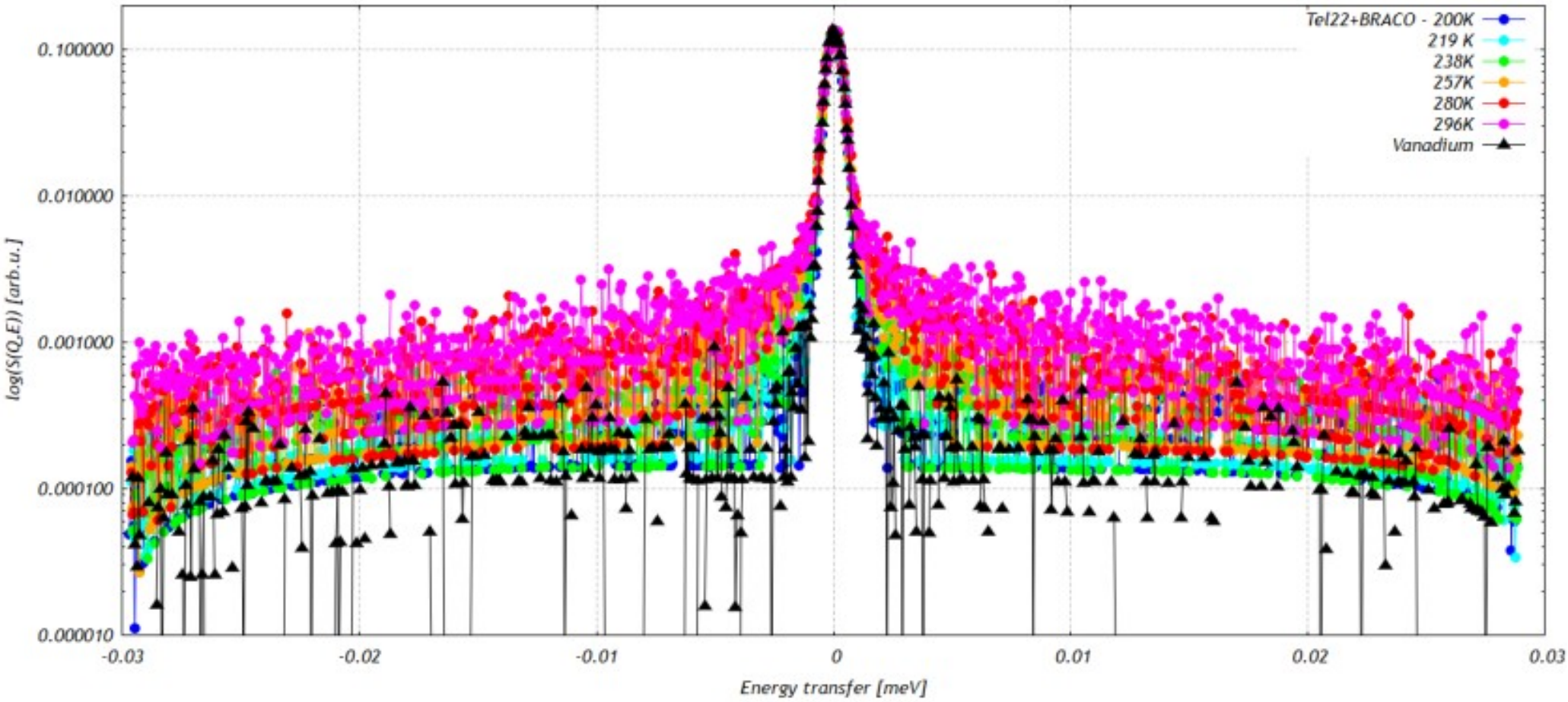

Tel22+BRACO19 QENS spectra at different temperatures

QENS spectra

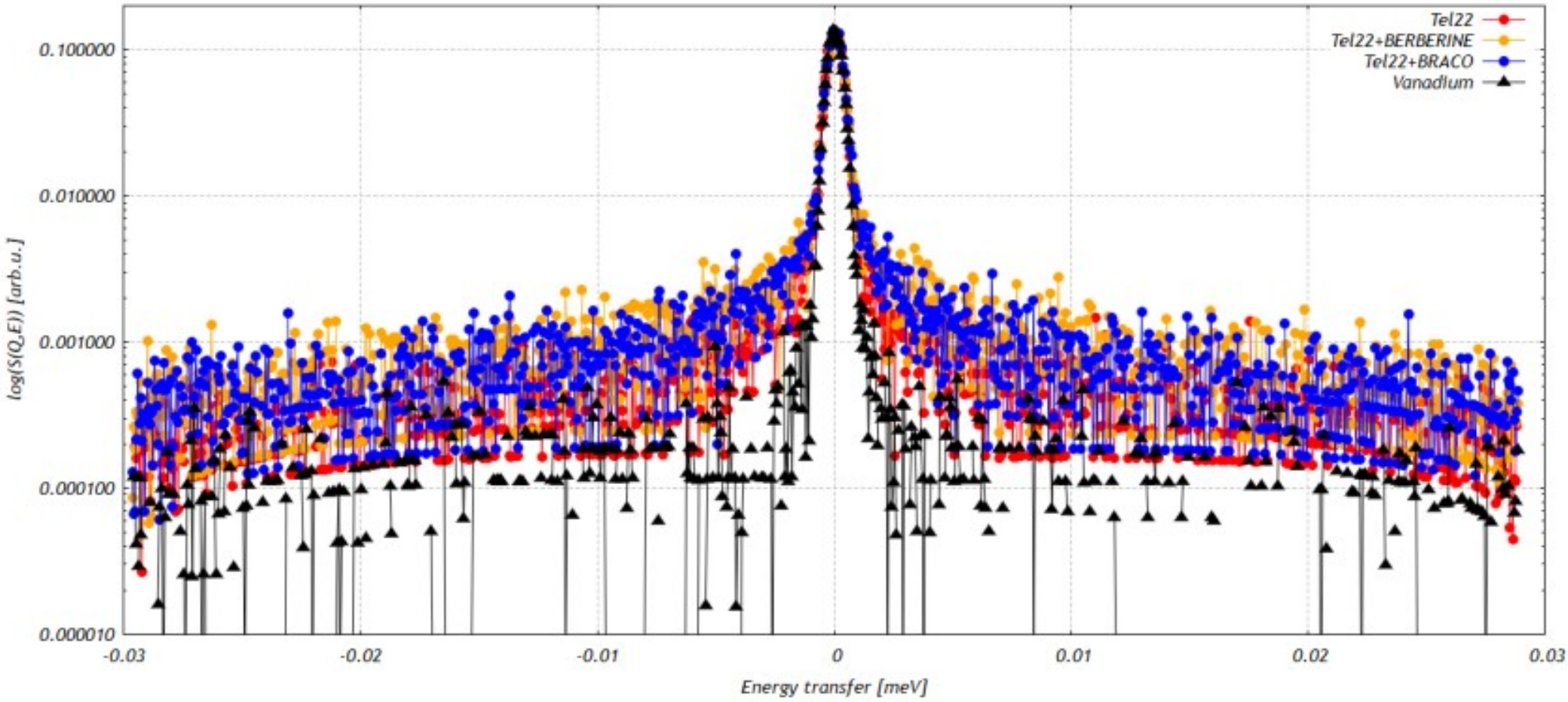

Comparison of the QENS spectra of the three samples at T=280K

QENS measurements: lorentzian broadening

Fitting function:

$$S(\vec{Q}, E) = W(\vec{Q})(a_0(\vec{Q})g(E) + (1 - a_0(\vec{Q}))V(E)) + B$$

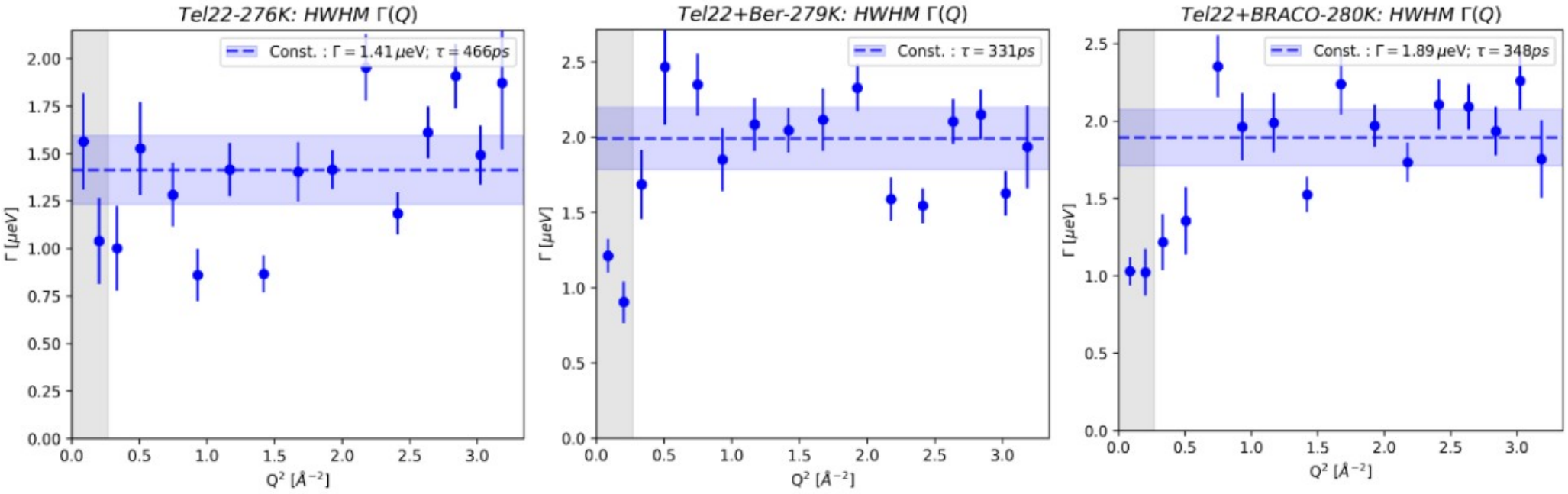

A constant fit to the FWHM also show that the broadening is increased upon complexation

QENS measurements: next steps

- Analysis of $a_0(Q)$ to determine the geometry of the confined motion;
- Implementation of a more complex fitting model;
- Analysis that takes into account also the dependence on the temperature of the fitted parameters.

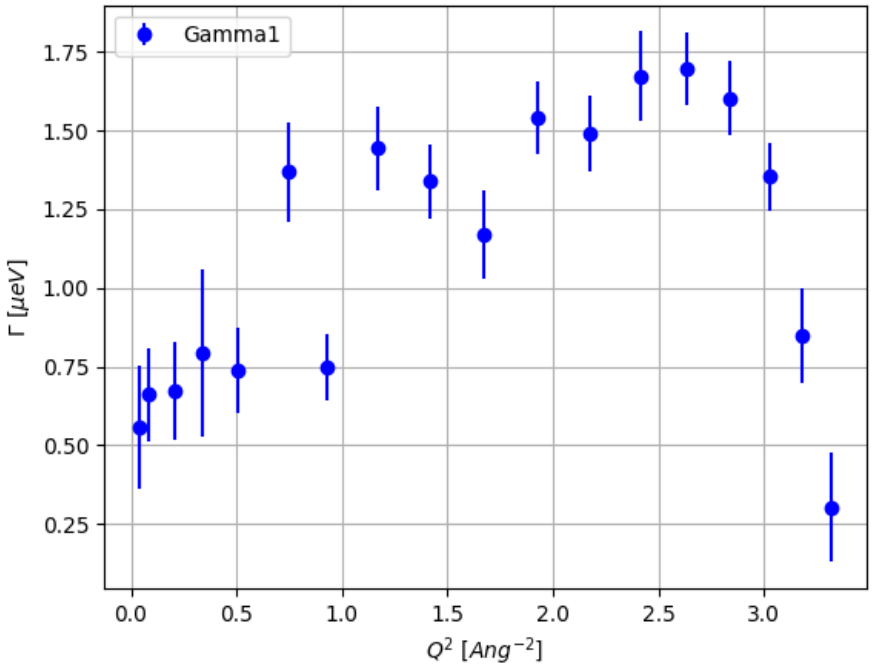

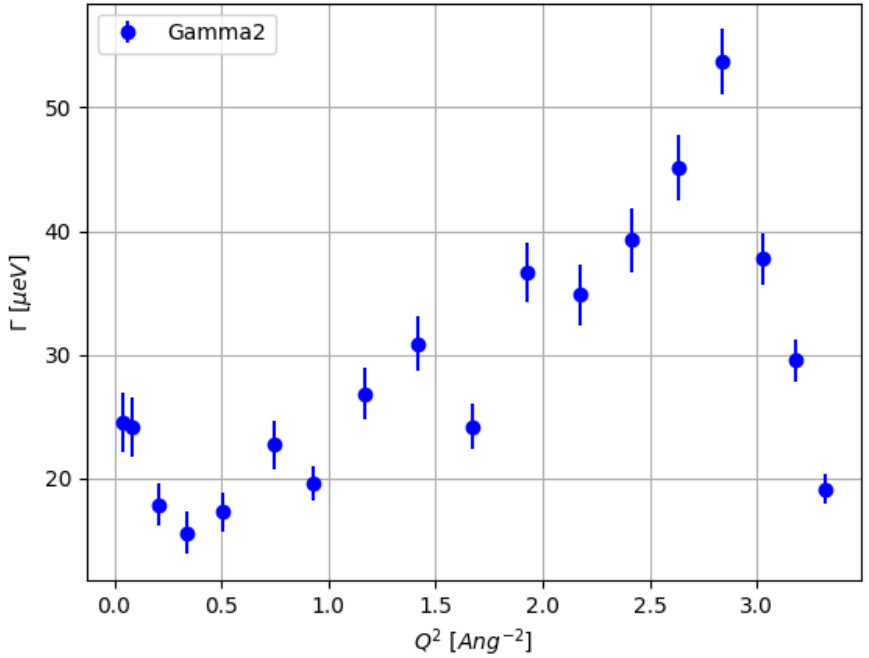

Lorentzian broadening as a function of Q^2 within a slightly more sofisticated model (two lorentzians) shows the signature of confined random-jump diffusion

QENS measurements: next steps

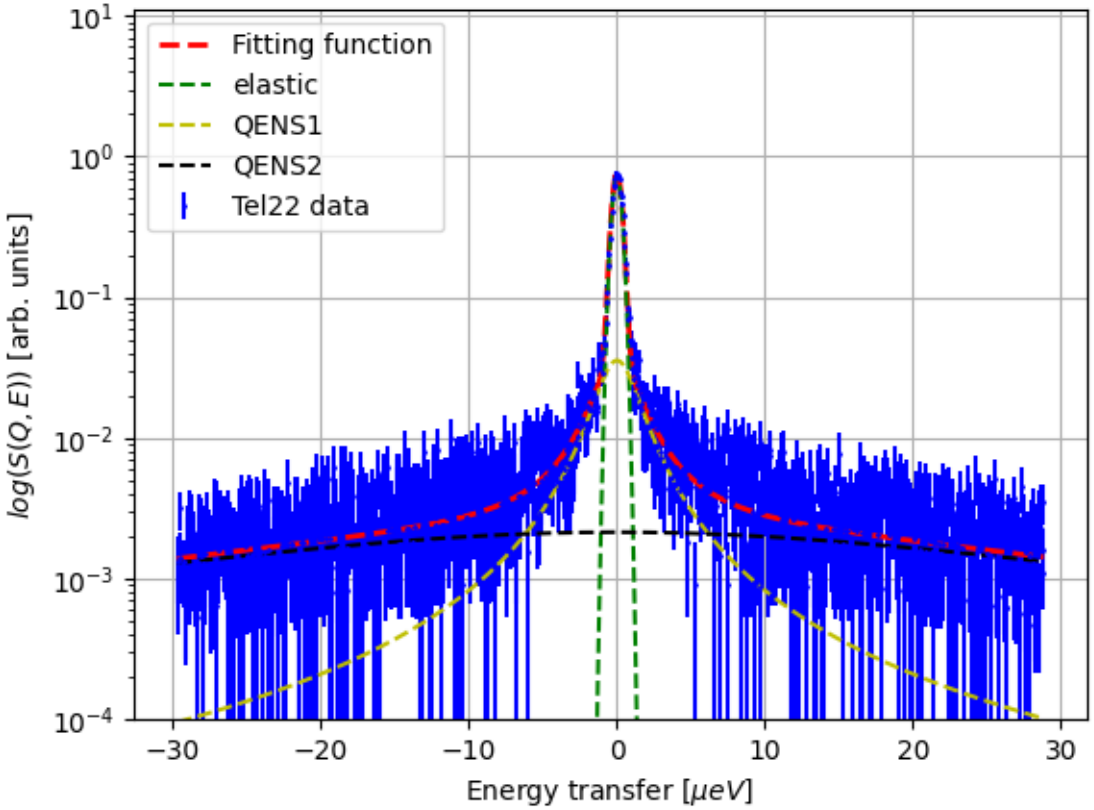

A QENS spectrum as fitted within a two-lorentzian functions

Thank you for your attention

References

- [1] Huppert JL, Balasubramanian S. G-quadruplexes in promoters throughout the human genome. Nucleic Acids Res. 2007;35(2):406-13. doi: 10.1093/nar/gkl1057. Epub 2006 Dec 14. Erratum in: Nucleic Acids Res. 2007;35(6):2105. PMID: 17169996; PMCID: PMC1802602.
- [2] Zhao C, Qin G, Niu J, Wang Z, Wang C, Ren J, Qu X. Targeting RNA G-Quadruplex in SARS-CoV-2: A Promising Therapeutic Target for COVID-19? Angew Chem Int Ed Engl. 2021 Jan 4;60(1):432-438. doi: 10.1002/anie.202011419. Epub 2020 Oct 27. PMID: 32939952.
- [3] Yu Z, Schonhoft JD, Dhakal S, Bajracharya R, Hegde R, Basu S, Mao H. ILPR G-quadruplexes formed in seconds demonstrate high mechanical stabilities. J Am Chem Soc. 2009 Feb 11;131(5):1876-82. doi: 10.1021/ja806782s. PMID: 19154151.
- [4] Fitter J. A measure of conformational entropy change during thermal protein unfolding using neutron spectroscopy. Biophys J. 2003 Jun;84(6):3924-30. doi: 10.1016/S0006-3495(03)75120-0. PMID: 12770898; PMCID: PMC1302974.